Astronomy & Astrophysics manuscript no. wang˙Muinonen˙paper1˙KM
January 24, 2013

Photometric analysis of the spin parameters and shapes for the C-type main-belt asteroids (171) Ophelia and (360) Carlova

Xiaobin Wang[1,2], Karri Muinonen[3], Tuomo Pieniluoma[3], Yibo Wang[1,2], Raoul Behrand[4], Rui Goncalves[5], Julian Oey[6], Pierre Antonini[7], Charistophe Demeautis[8], Federico Manzini[9], Jacques Damerdji[10], Jacques Montier[11], Alain Klorz[12,13], Arnaud Leroy[14], and Giller Ganand[14,]

[1] National Astronomical Observatories/Yunnan Observatory, CAS,P.O.Box 110,Kunming 650011, China.
e-mail: wangxb@ynao.ac.cn
[2] Key laboratory for the structure and evolution of celestial objects,CAS.
[3] Department of Physics, P.O. Box 64, FI-00014 University of Helsinki, Finland
e-mail: karri.muinonen@helsinki.fi
[4] Genève Observatory, 1290, Sauverny, Switzerland
[5] Linhaceira Observatorie, Instituto Politecnico de Tomar, Portugal
[6] Kingsgrove observatory,23 Monaro Ave., Kingsgrove, NSW, Australia
[7] Observatoire de Bédoin,47 rue Guillaume Puy,84000 Avignon, France
[8] Observatoire du Tim, Chemin La Chapelle, 04700 Puimichel, France
[9] Stazione Astronomica di Sozzago, Italy
[10] Institut d'Astrophysique et de Géophysique, Université de Liège, Belgium
[11] Center Astronomique de La Couyere, France
[12] Institut de Recherche en Astrophysique et Planétologie (IRAP), Université de Toulouse, 9 avenue du colonel Roche, 31028, Toulouse Cedex 4, France
[13] Observatoire de Haute-Provence, 04870 Saint Michell', Observatoire, France
[14] Observatoire Midi Pyrénes and Association T60, Pic du Midi, France

Received .... ??, 2012; accepted ..... ??, 2012

ABSTRACT

Context. Asteroids are thought to be remnants of planetesimals in the Solar System. Their physical parameters, such as the spin parameters and shapes, can provide important constraints on the formation and evolution of the entire Solar System as well as the individual small bodies themselves. The C-type asteroids are thought to be primitive small Solar System bodies, providing a particular reservoir of information on formation and evolution. In the present paper, the spin parameters and shapes of the C-type main-belt asteroids (171) Ophelia and (360) Carlova are analysed.

Aims. (171) Ophelia has been considered as a candidate binary system because of the eclipse features in the lightcurve obtained by E. Tedesco in 1979. Thereafter, numerous follow-up observations were carried out between 1977 and 2011 in order to confirm the binarity. Until now, no direct evidence has been obtained to verify the binarity of (171) Ophelia. In order to revisit the question of binarity, 40 lightcurves of (171) Ophelia are here analysed to determine its spin parameters and convex shape. (360) Carlova has been observed by several groups from 1977 to 2000, but they have reported inconsistent results for the spin period and pole orientation. Combining all published photometric data and new observed data of 2011 and 2012, the spin parameters and convex shape of (360) Carlova are analysed.

Methods. The shape and spin parameters of two C-type asteroids are determined from photometric data using the convex inversion method. Further, a novel virtual-photometry Monte Carlo method is applied to estimate the uncertainties of the spin parameters.

Results. Using the convex inversion method and the virtual-photometry Monte Carlo method, we derive a pair of possible poles for (171) Ophelia: $(152^{\circ}{}^{+1.3}_{-2.2}, +36^{\circ}{}^{+0.6}_{-5.8})$ for a prograde rotation state and $(317^{\circ}{}^{+2.2}_{-2.1}, +28^{\circ}{}^{+3.2}_{-3.9})$ for a retrograde rotation state with comparable rms values. The spin periods corresponding to the two poles are nearly the same: $6.665429^{+3.2(-6)}_{-1.5(-6)}$ hours (here, e.g., $+3.2(-6)$ stands for $+3.2 \times 10^{-6}$). The convex shape of (171) Ophelia shows binary characteristics. For (360) Carlova, a more accurate period of $6.189592^{+8.6(-7)}_{-1.5(-6)}$ hours is found. Similarly, we also find a pair of poles $(105^{\circ}{}^{+6.0}_{-2.7}, +61^{\circ}{}^{+3.7}_{-3.2})$ for a prograde rotation state and $(347^{\circ}{}^{+8.1}_{-4.7}, +60^{\circ}{}^{+4.5}_{-5.2})$ for a retrograde rotation state with comparable rms-values. The convex shape of (360) Carlova is roughly ellipsoidal. For both asteroids, the convex shapes corresponding to the pairs of poles are mirror images of each other.

Key words. asteroids; photometric data; spin period; pole orientation; shape

1. Introduction

The name "asteroid" was introduced for a particular class of small Solar System bodies because of their star-like appearance when observed with ground-based telescopes. Gradually, astronomers became aware of the irregular shapes of asteroids, although no shapes of asteroids were resolved in visible light before the Galileo spacecraft passed through the asteroid main belt. In the early stage of physical studies of asteroids, a simple triaxial ellipsoid model was often used. Assuming a triaxial ellipsoid shape for an asteroid allows for the inference of the pole orientation. For the asteroids of rubble-pile structure, the triaxial ellipsoid model can approximately represent

the shapes. But, for the asteroids of very irregular shape, the assumption of a triaxial ellipsoid introduce errors in the determination of the pole due to the large deviation of the model shape from the real shape of an asteroid. That constitutes one of the main reasons for the dispersion in pole determination when using different data sets, for example, data from different apparitations. Fortunately, a remedy was offered by the tireless efforts of numerous researchers (Russell 1906; Cellino et al. 1989; Karttunen1989; Karttunen&Bowell1989; Kaasalainen et al. 1992a; Kaasalainen et al. 1992b; Muinonen 1998; Muinonen & Lagerros 1998; Kaasalainen&Torppa 2001; and Kaasalainen et al. 2001). Now, several inversion methods are developed to determine the shape and spin parameters of asteroids, e.g., the convex inversion method (Kaasalainen&Torppa(2001) and Kaasalainen et al. 2001), which has been applied to more than one hundred asteroids in recent years.

Recent studies on the shape determination (e.g., Kaasalainen et al. 2002a, Torppa et al. 2003, Kaasalainen et al. 2004, Ďurech et al. 2009) have demonstrated that the convex inversion method can give reliable global shapes and more accurate spin parameters for main-belt asteroids (MBAs), near-Earth asteroids (NEAs), and Trojan asteroids from a varying combination of dense and sparse photometric data. However, error estimation for the convex inversion solution still constitutes a challenge. Kaasalainen et al. (2001) and Torppa et al. (2003) estimated the errors for the pole orientation by the longitude and latitude distributions generated by varying the initial values of parameters and the scattering models. They derived steep distributions, even though such distributions can be considered unrealistic. Hanuš et al. (2011) gave a typical uncertainty value of $\pm 10^{\circ}$ for pole solutions by investigating the pole distribution derived from the what they called "mock" objects. For the spin period, they all gave an uncertainty of $0.01 - 0.1$ times the "basic resolution interval" (see the definition in Kaasalainen et al. (2001). In the present paper, we apply the convex inversion method to solve for the spin parameters and shapes of the C-type main-belt asteroids (171) Ophelia and (360) Carlova, as well as apply a novel virtual-photometry Monte Carlo method (cf. Muinonen et al. 2012) to obtain tentative estimates for the uncertainties of the poles and spin periods.

Tedesco (1979) observed (171) Ophelia in 1977, and suggested that it could be a synchronous binary asteroid system based on the V-shaped lightcurve minimum (similar to an eclipsing feature in binary stars). In order to verify the suggestion, several groups made follow-up observations with various techniques, e.g., stellar occultations, as well as photometric and spectroscopic methods. We obtained photometric observations with a 1-meter telescope for (171) Ophelia in four nights in 2003, and found that the lightcurves show the two normal peaks of sinusoidal shape instead of the V-shape minima. Between the period of 2005 and 2011, nine other groups also obtained photometric observations for (171) Ophelia. Among those observations, some lightcurves repeated the feature of the V-shape minimum. However, no other direct evidence confirms the binarity of (171) Ophelia except the V-shape minima of the lightcurves, and also no pole orientation and shape information have been derived until now. As a first step toward unveiling the nature of (171) Ophelia, we will here solve for the spin parameters and convex shape with the convex inversion method, and give the error estimates for spin parameters with the virtual-photometry Monte Carlo method.

Several groups have carried out photometric observations for (360) Carlova since 1979, but they have reported inconsistent spin period and pole orientation results. Harris & Young(1983) gave a period of 6.21 hours from their four nights of photometric data in 1979. Di Martino et al. (1987) reported a period of 6.183 hours with their two nights of data obtained in 1984. Dotto et al. (1995) estimated the triaxial ellipsoid shape and pole orientation for (360) Carlova with the one night of photometric data obtained on 9 Jan. 1986 and previously published data (Harris & Young 1983,Di Martino et al. 1987), and derived a pair of poles: (108°,51°) (in ecliptic coordinates) with the axial ratio of $a/b = 1.56$ and $b/c = 1.0$; and (337°,47°) with $a/b = 1.58$ and $b/c = 1.0$, respectively. Michalowski et al. (2000) suggested a period of 6.188 hours with their seven nights of photometric data obtained in 1996, 1997, and 1998. Using the Epoch method, Wang & Zhang(2006) analysed the spin parameters of (360) Carlova with 12 lightcurves (one obtained by them on 15 Nov. 2000 and the other 11 collected from the literature), and estimated a pole of (95°, 40°) with a spin period of 6.1873 hours. In order to re-determine the spin parameters, we performed another nine nights of photometric observations in 2011 and 2012. Together with 14 previously published lightcurves, the spin parameters and convex shape of (360) Carolova are analysed in this paper.

The observations and data reduction for the C-type asteroids (360) Carlova and (171) Ophelia are presented in section 2. The solutions from convex inversion for (171) Ophelia and (360) Carlova are shown in section 3. In section 4, the virtual-photometry Monte Carlo method is applied to estimate the uncertainties of spin parameters for two selected targets. The last section gives the primary conclusions.

2. Observation and Data Reduction

Asteroid (171) Ophelia is a C-type main-belt object with a diameter of 115 km. It is one of the core members of the Themis family, in which the binary system (90) Antiope and the multiple system (379) Huenna are confirmed. As a potential binary system, (171) Ophelia is an interesting object to be studied. As a whole, 39 unpublished lightcurves of (171) Ophelia are included in the present analysis. Four of these lightcurves have been obtained by ourselves, and the rest come from the Asteroids and Comets Rotation Curves, CdR (`http://obswww.unige.ch/~behrend/page_cou.html`) which is a database maintained by R. Behrend.

Photometric observations for (171) Ophelia were carried out on four nights (November 25 and 30, 2003, as well as December 1 and 2, 2003) with a 1.0-meter telescope at the Yunnan observatory, China. A $1k \times 1k$ CCD camera with a field of view of $6'.5 \times 6'.5$ was used to gather the data through the R filter. The 35 additional new lightcurves of (171) Ophelia used in this paper were obtained by nine groups: (a) Rui Goncalves (9 lightcurves without filter and 2 lightcurves in the R-band); (b) Juliane Oey (6 lightcurves in the R band); (c) Pierre Antonini (5 lightcurves in the R-band); (d) Charistophe Demeautis (3 lightcurves in the B-band and 2 lightcurves in the V-band); (e) Yassine Damerdji (2 lightcurves in the R-band); (f) Jacques Montier (2 lightcurves in the V-band); (g) Federico Manzini (2 lightcurves in the R-band); (h) Alain Klorz and Raoul Behrand (1 lightcurve in the R-band); and (i) Arnaud Leroy and Giller Canand (1 lightcurve in the V-band). Additionally, one published lightcurve (Tedesco 1979) of (171) Ophelia is also included here. The whole data set spans 34 years, most of the data obtained between 2003 and 2011. The detailed observational information of (171) Ophelia is listed in Table 1.

Asteroid (360) Carlova is a C-type main-belt asteroid with a diameter of 138 km. It was discovered by Auguste Charlois

on 11 March 1893 in Nice. In the present paper, 15 nights of published photometric data of (360) Carlova obtained between 1977 and 2000 are included. New photometric observations for (360) Carlova were made in 2011 and 2012 with the 1.0-meter telescope and a $2k \times 2k$-pixel Andor DW436 CCD at the Yunnan Observatory, China. The field of view of the 2k CCD camera is $7'.3 \times 7'.3$. In all nine nights, photometric data were obtained through a clear filter or a R-filter depending on the weather conditions. Information for all the photometric data of (360) Carlova included in the paper are listed in Table 1.

With the IRAF [1] software, the bias effect on the scientific images was subtracted by an averaged bias-image, and the flat-field correction was carried out by dividing with a weighted and averaged flat-field image. The dark currents of the two CCD detectors are small, so the corresponding corrections are neglected. The random cosmic-ray hits in the images are identified by a threshold of four times the standard deviation of the background, and they are removed. The instrumental magnitudes of the celestial objects in the images are measured using the aperture photometry task in the IRAF software with an optimal aperture size. The magnitude differences for an asteroid are calculated comparing to one or several reference stars in the same image. The time stamps of all involved observations are corrected by the light time and then converted into JD in TDB time system.

For the new magnitudes of (360) Carlova in 2011 and 2012, we applied the coarse de-correlation method (Collier et al. 2006) and Tamuz's method (Tamuz et al. 2005) to correct for the systematic errors in the photometric data. The latter method was originally developed for increasing the signal-to-noise ratio of exoplanet transits. The systematic errors were modeled, firstly, with all stable reference stars in the images, then those modeled systematic errors are removed from the photometric data of the asteroid. Therefore, the errors in the lightcurves of each night were significantly decreased (Wang et al. 2010).

Before convex inversion for asteroid spins and shapes, the absolute magnitudes and/or relative magnitudes of the asteroids need to be converted into fluxes. Here, we firstly reduced the absolute magnitudes through different filters into the V-band magnitude according to the color indices, and then converted them into absolute fluxes according to Vega's flux in the V-band:

$$\begin{aligned} L_{\mathrm{abs\_}v} &= 10^{-0.4M_v} L_{\mathrm{Vega\_}v}, \\ L_{\mathrm{Vega\_}v} &= 3631\mathrm{Jy}. \end{aligned} \quad (1)$$

Here M_v represents the absolute magnitude in the V-band. $L_{\mathrm{Vega\_}v}$ is the flux of Vega in the V-band corresponding to the zero point of the visible magnitude system.

For the case of relative magnitudes, the relative fluxes of the targets are computed from

$$L_{\mathrm{rel}} = 10^{-0.4(M-\bar{M})}. \quad (2)$$

Here M refers to the relative magnitudes of the asteroid. $\bar{M}$ denotes the mean value of each lightcurve. The lightcurves (as relative magnitudes) of (171) Ophelia and (360) Carlova are shown in Figs. 1 and 2, respectively.

3. Determination of spin and shape

The convex inversion method can yield complete information on the spin and shape of an asteroid from the lightcurves. It has been applied to main-belt (e.g., Torppa et al. 2003 and 2008), near-Earth (Kaasalainen et al. 2004) and Trojan asteroids. Here we apply the method to solve for the spin parameters and the shape of the C-type main-belt asteroids (171) Ophelia and (360) Carlova.

The convex inversion method is described in detail by Kaasalainen & Torppa (2001) and Kaasalainen et al. (2001). Here the procedure for the determination of the spin parameters and the shape of the two selected asteroids with the convex inversion method is briefly summarized. The convex inversion method finds a shape and spin state corresponding to the minimum rms-value σ_{rms} between the observed and model brightnesses:

$$\sigma_{\mathrm{rms}} = \sqrt{\tfrac{1}{n}\sum_{j=1}^{n}\left\|L^j_{\mathrm{obs}} - L^j_{\mathrm{mod}}\right\|^2}. \quad (3)$$

Here L^j_{obs} is the j^{th} observed absolute or relative brightness of an asteroid. L^j_{mod}, the model brightness, is the sum of the observable brightnesses due to the illuminated surface elements of the asteroid. In other words, the model brightness of the asteroid is associated with the scattering law of the surface, as well as the surface elements illuminated by the Sun and observable by the observers:

$$\begin{aligned} L_{\mathrm{mod}} &= \textstyle\sum_i S(\mu,\mu_0,\alpha) G(\vartheta_i,\psi_i)\sigma_i, \\ S(\mu,\mu_0,\alpha) &= f(\alpha)\mu\mu_0(\tfrac{1}{\mu+\mu_0}+c), \\ G(\vartheta_i,\psi_i) &= exp(\textstyle\sum_{lm} a_{lm} Y_l^m(\vartheta_i,\psi_i)). \end{aligned} \quad (4)$$

$S(\mu,\mu_0,\alpha)$ (cf. Equation 3 in Kaasalainen et al. 2001) represents the scattering law of an asteroid's surface, composed of the Lommel-seeliger law, the Lambert law and the phase function. The weight factor c balances the two laws depending on the surface material of the asteroid. μ is the cosine of the angle between the normal vector of the i^{th} facet and the line of sight, μ_0 is the cosine of the angle between the normal vector of the i^{th} facet and the source of light. $G(\vartheta_i,\psi_i)$ is the Gaussian surface density of the asteroid in the normal coordinates (ϑ_i,ψ_i), and the σ_i is the facet area on a triangulated unit sphere. Therefore, the size of the i^{th} facet on the triangulated surface of the asteroid is given by $G(\vartheta_i,\psi_i)\sigma_i$. In the present implementation of convex inversion, $G(\vartheta_i,\psi_i)$ is represented with an exponential spherical harmonics series, which ensures the positivity of the Gaussian density of a shape. In other words, it enforces a convex shape for the asteroid. Because the normal vectors of a convex surface are determined unambiguously, it is more easy to derive a unique shape solution for an asteroid from photometric data. For a non-convex asteroid, a convex shape is derived, wrapping the natural shape. In that case, facets with large areas may represent those potential non-convex features on the asteroid's surface.

In practical modelling, the shape of an asteroid is represented with a truncated series of spherical harmonics due to the limited accuracy of ground-based photometric data. Since only relative intensities are involved in the convex inversion for the two asteroids, the parameters related to the scattering law are fixed. In detail, the parameters of the phase function are: $a = 0.5$, $d = 0.1$ and $k = -0.5$, and the weight factor c is set at $c = 0.1$. The unknown parameters (coefficients of the spherical harmonics series as well as the spin period and pole orientation) can be solved with the Levenberg-Marquardt method by minimizing σ_{rms}. Everyone knows that the Levenberg-Marquardt method (a nonlinear square least method) searches for a minimum of rms along the gradient direction starting from certain initial values of parameters. Sometimes, the search converges into a local minimum. Therefore, a range of initial values are needed to search for

[1] IRAF is distributed by the National Optical Astronomy Observatories, which are operated by the Association of Universities for Research in Astronomy, Inc., under cooperative agreement with the National Science Foundation.

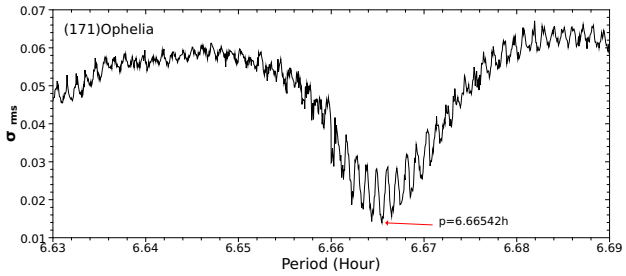

Fig. 1. The spin period distribution of (171) Ophelia vs. the rms-value of the fit.

the global minimum. In our analysis, a wide range of spin period is scanned with a reasonable sampling step in order to find the best spin period, and only some initial poles are tested. During the scanning procedure of the period, lower-degree spherical-harmonics series are included in order to speed up the computations. Then, higher-order spherical-harmonics series are involved after having found the spin period. In what follows, inversion results are described for (171) Ophelia and (360) Carlova.

3.1. (171) Ophelia

For (171) Ophelia, 40 lightcurves are used to determine its spin parameters and shape with the convex inversion method. Among those lightcurves, only a single lightcurve has been published before (Tedesco 1979). The entire data set spans 32 years, with the solar phase angle varying from 1°.4 to 21°.

Tedesco (1979) obtained a lightcurve with a V-shaped minimum (see Fig. 6), and reported a spin period of 6.672 h. Here an interval of the spin period between 6.63 h to 6.69 h is scanned with a sampling step of $0.8\Delta p$ (with Δp defined according to Eq. 2 in Kaasalainen et al. 2001). Figure 1 shows the distribution of the spin period vs $\sigma_{\rm rms}$. The most significant minimum is found around 6.665422 h. The value is slightly smaller than that by Tedesco (1979). With this period as a new initial value, the pole and the shape parameters–spherical harmonics coefficients up to degree $l = 8$ are modelled numerous times with different initial values of pole orientation. Finally, a pair of pole solutions is found at (152°, +36°) and (317°, +28°) in ecliptic coordinates (J2000) and the solutions have a comparable rms-value of $\sigma_{\rm rms} = 0.012$. For the two pole candidates, the spin period is nearly the same.

The shapes corresponding to the two poles are mirror images of each other (see Fig. 2). The convex modeling of (171) Ophelia suggests a binary structure, in resemblance to the convex models of (41) Daphne and (44) Nysa (Kaasalainen et al. 2002b). Additionally, we have computed approximate relative triaxial dimensions as defined in Kaasalainen et al. (2002a) and in Torppa et al. (2008). In the former approach, the dimensions represent certain averages of overall dimensions and dimensions obtained from a specific triaxial ellipsoid fit; whereas, in the latter approach, an alternative triaxial ellipsoid fit is utilized. These two sets of dimensions, as well as their averages, are given in Table 2. We note that the axial ratios a/b corresponding to two pole solutions are similar, whereas the axial ratios b/c show a small deviation. This deviation may rise from the large uncertainty in the facet areas near the poles due to the limited observational coverage. The goodness of the modeled brightness of (171) Ophelia can be seen Fig. 3.

Table 2. The relative triaxial dimensions for the convex shape models of (171) Ophelia. We give the axial ratios due to the definitions by Kaasalainen et al. (2002a; column 2) and by Torppa et al. (2008; column 3), as well as their average (column 4).

Pole, Period	Dimensions I	Dimensions II	Mean
(152°, +36°)	$a/b = 1.23$	$a/b = 1.23$	$a/b = 1.23$
6.665429 h	$b/c = 1.20$	$b/c = 1.19$	$b/c = 1.20$
(317°, +28°)	$a/b = 1.20$	$a/b = 1.23$	$a/b = 1.22$
6.665429 h	$b/c = 1.27$	$b/c = 1.26$	$b/c = 1.27$

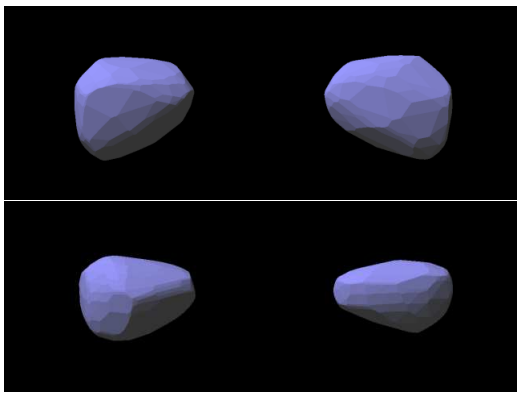

Fig. 2. The convex shape of (171) Ophelia. The upper plots correspond to the pole-on view and the bottom plots to the equatorial view. Shapes are depicted for two pole solutions: (152°, 36°) (left) and (317°, 28°) (right).

3.2. (360) Carlova

For (360) Carlova, 23 lightcurves are used in the convex inversion. Among those lightcurves, 9 lightcurves observed in 2011 and 2012 are new and the rest are from Harris&Young (1983), di Martino et al. (1987), Dotto et al. (1995), Michalowski et al.(2000), and Wang&Zhang(2006). The full data set spans 34 years (from 1979 to 2012), and the solar phase angle varies from 5° to 22°. The photometric data are used with equal weights in the convex inversion because of missing error information for the collected lightcurves.

The spin parameters and the triaxial ellipsoidal shape of (360) Carlova have been studied by several groups, but the previous results using different data sets or different analysis techniques have been inconsistent. Here, we re-analyze the spin parameters and the shape for (360) Carlova using the convex inversion method based on the previously existing and newly observed data. The interval of spin period between 6.15 h to 6.3 h is scanned with a sampling step of $0.8\Delta p$. A significant rms minimum is found around 6.189593 h (see the upper plot of Fig. 4). We also note that some local minima, for example, 6.183 h, 6.187 h, 6.1886 h, and 6.2 h coincide with the previous published values for the period (see the bottom plot of Fig. 4).

With the scanned spin period as the new intial value, the shape inversion procedures are run again with the spherical-harmonics coefficients up to the degree $l = 8$. In order to find the global rms minimum, different initial values of pole orientation were tested. A pair of pole solutions of $(105°, 61°)$ and $(338°, 60°)$ are found with the nearly the same rms-value. The spin periods corresponding to the two poles are nearly the same, that is, 6.189593 h. Figure 5 shows the convex shapes of (360) Carlova for the two poles. The two shapes in pole-on view (the upper plots of Fig. 5) are mirror images of each other. Figure 6 shows the observed and modeled lightcurves. As a sim-

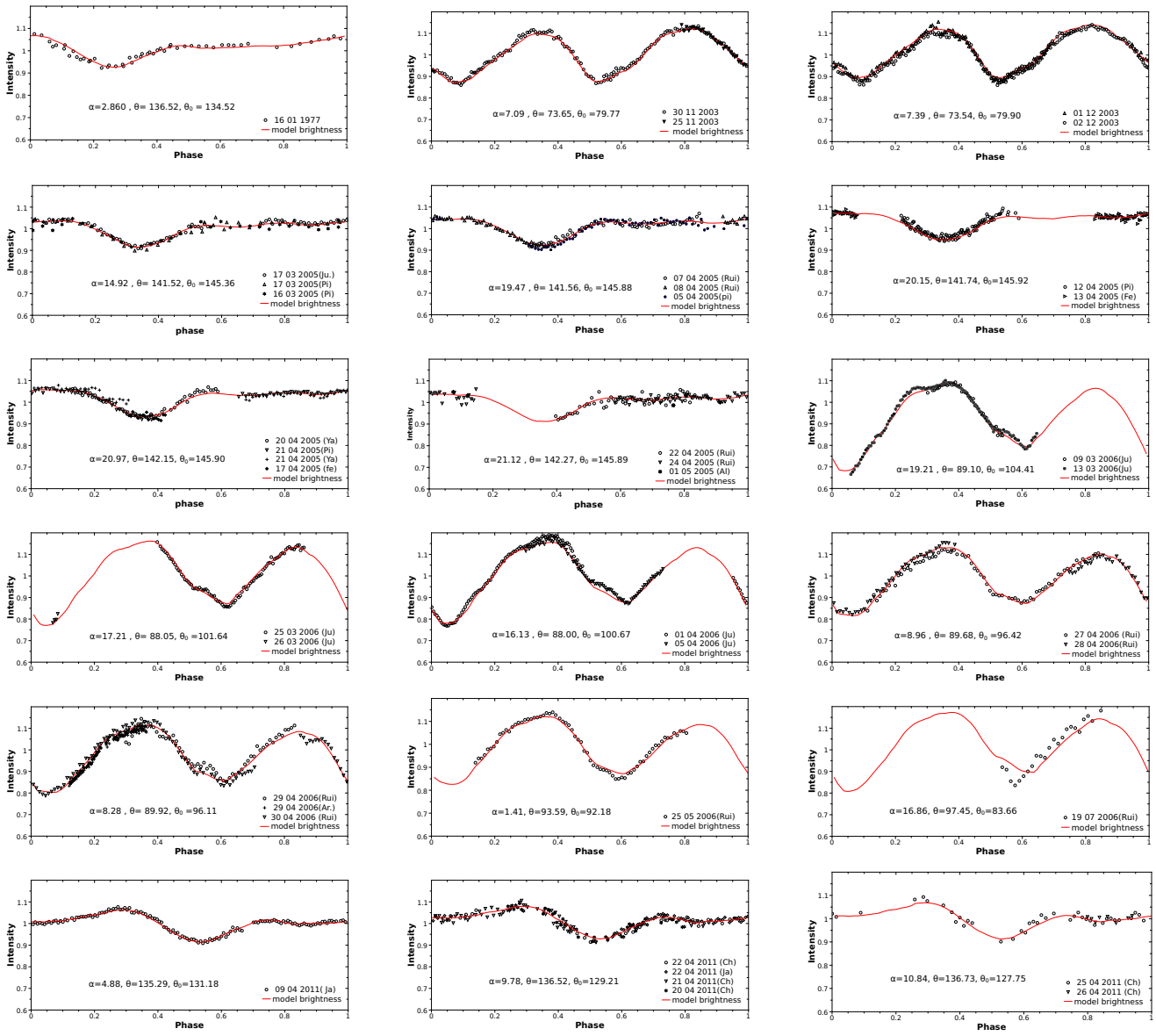

Fig. 3. The lightcurves for (171) Ophelia folded with the period of 6.665429 h.

ply comparison of the shapes corresponding to the two poles, we have computed their approximate relative triaxial dimensions (Table 3), and found that they are close to one another for a/b and differ slightly for b/c.

Table 3. As in Table 2 for (360) Carlova.

Pole, Period	Dimensions I	Dimensions II	Mean
(105°, +61°)	a/b = 1.26	a/b = 1.31	a/b = 1.29
6.189592 h	b/c = 1.49	b/c = 1.56	b/c = 1.54
(338°, +60°)	a/b = 1.29	a/b = 1.25	a/b = 1.27
6.189592 h	b/c = 1.63	b/c = 1.69	b/c = 1.66

4. Error estimation for the spin parameters

Kaasalainen et al. (2001) and Torppa et al. (2003) estimated the uncertainties of the pole and period by investigating the distribution of the parameters generated through varying the initial values of the parameters and the scattering models. Torppa et al. (2003) found that the distributions were usually steep and that the errors estimated from those distributions (e.g., typical errors of ±2° for the pole) are less realistic. More realistic uncertainties of 10° (twice the uncertainty of ±5° stated in Kaasalainen & Torppa 2001) for the pole were suggested. In both works, $0.01\Delta p - 0.1\Delta p$ was taken as the basic uncertainty of the spin period. Hanuš et al. (2011) estimated the uncertainties of the spin parameter with the distribution of parameters generated by different 'mock' objects, and gave a typical uncertainty of 10° of the pole.

In order to estimate the uncertainties in convex inversion, a novel virtual-observation Markov-chain Monte Carlo method (MCMC-V) described by Muinonen et al. (2012) can be used. For the present inverse problem, MCMC-V entails the following steps. Numbers of virtual photometric data sets are generated by adding Gaussian random noise to the original photometric data. The respective virtual least-squares solutions of convex inversion constitute a certain distribution of the unknown parameters. Convolution of this distribution by itself then provides a

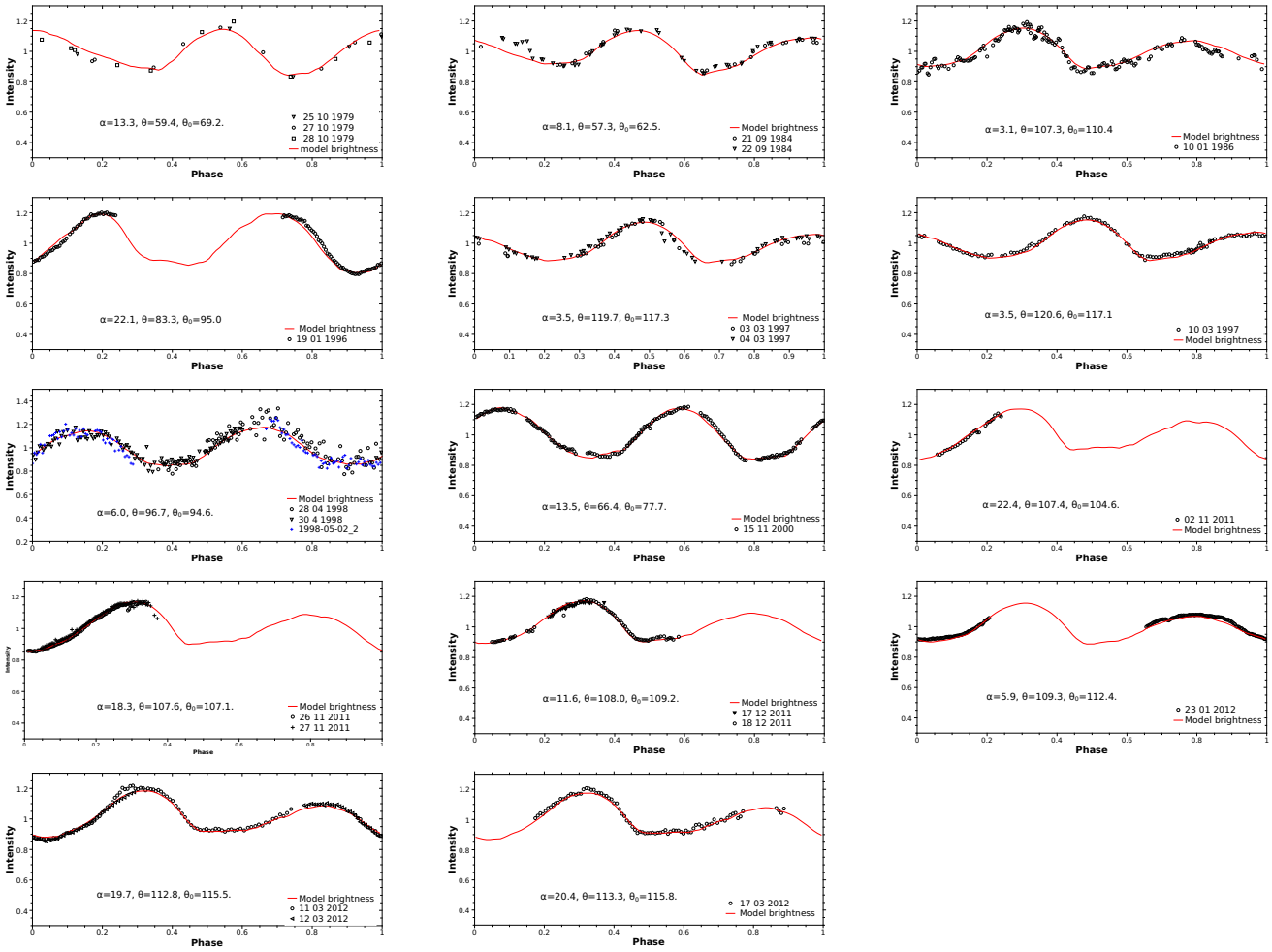

Fig. 6. The lightcurves of (360) Carlova folded with the period of 6.189592 h.

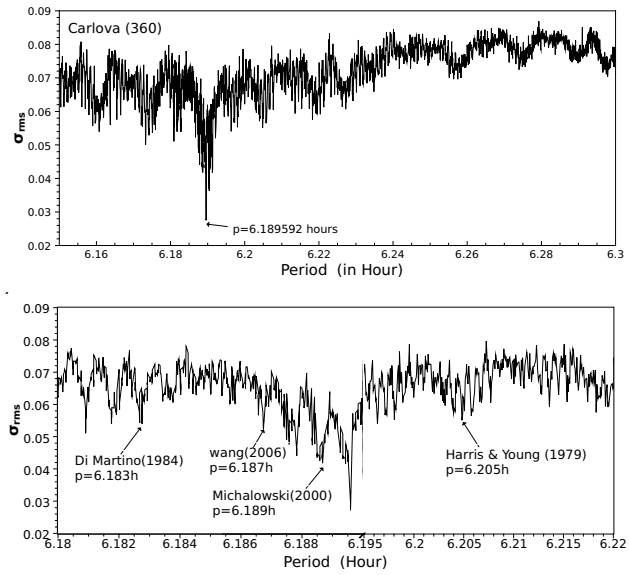

Fig. 4. The period distribution of (360) Carlova vs. the rms-value of the fit.

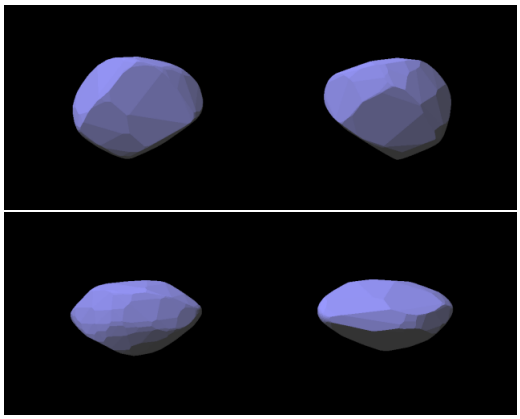

Fig. 5. The convex shape of (360) Carlova. The upper plots correspond to the pole-on view and the bottom plots to the equatorial view. Shapes are depicted for two pole solutions: $(105°, 61°)$ (left) and $(338°, 60°)$ (right).

symmetric proposal distribution for a random-walk Metropolis-Hastings algorithm. A full MCMC treatment of convex inversion then follows and results in a joint distribution of the spin and shape parameters. In the present context, we follow an approximate approach by obtaining rough error estimates using the virtual least-squares solutions described above.

Based on the distributions of the virtual least-squares solutions, uncertainties for spin period and pole are estimated with statistical methods. For a standard normal distribution, the center value X_c and half width w of the distribution can be taken as

the most likely value and the uncertainty for a parameter. But as the distribution can be asymmetric, we take the mode value as the most likely value for the unknown parameter and give the $1-\sigma$ limits (the 15.85 and 84.15 percentage bounds) as the uncertainty of parameter. Here, we estimate the uncertainties of the pole and period for (171) Ophelia and (360) Carlova.

Based on the photometric data of (171) Ophelia, 1000 virtual observational data sets were generated by adding random Gaussian noise of a standard deviation of 0.05 mag. Then, the distributions for the parameter values were derived with the respective virtual least-squares solutions. It took nearly 17 hours to find the 1000 least-squares soluions for (171) Ophelia, and in all 34 hours is needed to get the pair of poles candidates. Figure 7 shows the histrograms for the pole and period of (171) Ophelia, the line representing the Gaussian fit for the distribution. From Fig. 7, it is evident that the distributions deviate from the Gaussian distribution. As a comparison, the uncertainities of the pole and period given by the Gaussian fit and the $1-\sigma$ limits of the distribution are as follows: a pole value of $(151^\circ \pm 1.7, +33^\circ \pm 3.4)$ with a period of 6.6654265 ± 0.0000013 h given by the Gaussian fit and a pole value of $(152^{\circ}{}^{+1.3}_{-2.2}, +36^{\circ}{}^{+0.6}_{-5.8})$ with a period of $6.665428^{+0.00000023}_{-0.0000031}$ h given by the mode and the $1-\sigma$ limits of the distribution. Considering the shape of the distribution, the error estimates with the $1-\sigma$ limits of the distribution are more realistic. Following the approach based on the mode and the $1-\sigma$ limits, the other pole candidate for (171) Ophelia is $(317^{\circ}{}^{+2.2}_{-2.1}, +28^{\circ}{}^{+3.1}_{-3.9})$ with a period of $6.665428^{+0.0000042}_{-0.00000053}$ hours.

For the asteroid (360) Carlova, 1000 virtual photometric data sets were generated by adding random Gaussian noise with a standard deviation of 0.05 mag to the original photometric data. The distributions of the pole and period values were derived with 1000 sets of virtual least-squares solution (see Fig. 8). It took nearly 16 hours to find the 1000 least-squares soluions for (360) Carlova, and in all 32 hours is needed to get the pair of poles candidates. With the mode analysis and $1-\sigma$ limits of the distribution, we derived a pole of $(105^{\circ}{}^{+6.0}_{-2.7}, +61^{\circ}{}^{+3.7}_{-3.2})$ with a period of $6.189592^{+0.00000085}_{-0.00000068}$ h. For the another candidate pole, the median value and $1-\sigma$ limits of distribution are used because of two peaks distribution, that is $(347^{\circ}{}^{+8.1}_{-4.7}, +60^{\circ}{}^{+4.5}_{5.2})$ with a peroid of $6.189591^{+0.00000186}_{-0.00000058}$ h.

For the virtual shapes derived with the virtual photometric data, we investigated the size distribution of each facets. We found that the size distribution of the facets near the equatorial region have a narrow Gaussian distribution, while the distribution of the facets near the pole regions have a relatively wide distribution and sometime with some outliers. The wide distributions in the polar region are the reason for the large shape uncertainties of along the shortest axis dimension.

5. Discussion

Using the convex inversion method, the spin parameters and shapes of the two C-type asteroids (171)Ophelia and (360)Carlova were analysed from their photometric data. Furthermore, a noval virtual photometric Monte Carlo method was used to estimate the uncertainties of the spin parameters: in all cases, these uncertainties turned ut to be realistic.

The modeled convex shape of (171) Ophelia shows a binary structure, which resembles that of (41) Daphne and (44) Nysa. In the figure 9, we presents the convex shapes of these three binary structure asteroids. The second and third raws of figure 9 are the convex shapes of (41) Daphne and (44) Nysa given by Kaasalainen et al.(2002b). And the first raw shows the convex

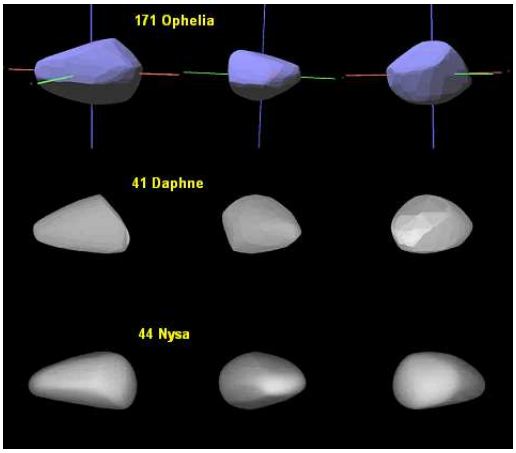

Fig. 9. The convex shape of (171) Ophelia, (41) Daphne and (44) Nysa, three figures are 120° apart in rotational phase.The covex shape of (171) Ophelia is for the pole 1,)

shapes of (171) Ophelia, viewed from three equator-edge directions of 120° rotational phase apart (same as the phase apart of (41) Daphne and (44) Nysa).

The approximate relative triaxial dimensions of the shape of (171) Ophelia for the two poles are: $a/b = 1.23$, $b/c = 1.19$ and $a/b = 1.22$, $b/c = 1.27$, respectively. For the asteroids (41) Daphne and (44) Nysa, we also computed the approximate relative triaxial dimensions based on the shape data provided by Database of Asteroid Models from Inversion Techniques(DAMIT) (Ďurech et al.2010). We found that the ratio a/b both of (41)Daphne and (44) Nysa are larger than that of (171) Ophelia, while the ratio a/c of three asteroids are roughly close. The relative axial ratios of three asteroids by fiting a triaxial ellipsoid and measuring the overall dimentsion are listed in Table 4

Table 4. As in Table 2 for three binary stucture asteroids (171)Ophelia, (41)Daphna and (44)Nysa.The values of (171)Ophelia is that for pole 1

Asteroid	Dimensions I	Dimensions II	Mean
(171)Ophelia	$a/b = 1.23$	$a/b = 1.23$	$a/b = 1.23$
Pole 1	$b/c = 1.20$	$b/c = 1.19$	$b/c = 1.20$
	$a/c = 1.48$	$a/c = 1.48$	$a/c = 1.48$
	$a/b = 1.20$	$a/b = 1.23$	$a/b = 1.22$
Pole 2	$b/c = 1.27$	$b/c = 1.26$	$b/c = 1.27$
	$a/c = 1.53$	$a/c = 1.55$	$a/c = 1.54$
(41) Daphna	$a/b = 1.34$	$a/b = 1.26$	$a/b = 1.30$
	$b/c = 1.11$	$b/c = 1.16$	$b/c = 1.14$
	$a/c = 1.49$	$a/c = 1.45$	$a/c = 1.47$
(44) Nysa	$a/b = 1.34$	$a/b = 1.31$	$a/b = 1.33$
	$b/c = 1.13$	$b/c = 1.18$	$b/c = 1.15$
	$a/c = 1.52$	$a/c = 1.55$	$a/c = 1.53$

For (360) Carlova, we found the best spin period of $6.189592^{+0.00000086}_{-0.0000015}$ h based on 23 nights of photometric data, and derived a pair of candidate poles: $(105^{\circ}{}^{+6.0}_{-2.7}, +61^{\circ}{}^{+3.7}_{-3.2})$ and $(347^{\circ}{}^{+8.1}_{-4.7}, +60^{\circ}{}^{+4.5}_{5.2})$. It is important that the pole latitude value of 60° follows accurately with an uncertainty of 5°. The new derived latitude of pole of (360) Carlova is larger than the previous published values. The uncertainty of second pole is larger than that of first pole, and more complicately, the distributions of second pole foucs on two regions around $(347°, +64°)$ and $(356°, +56°)$ (see Fig. 10).

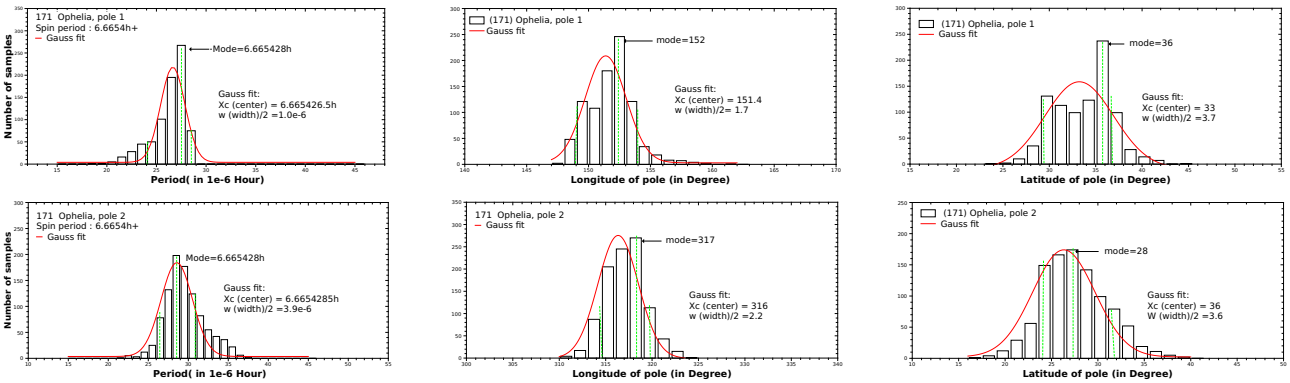

Fig. 7. The spin-parameter distributions for (171) Ophelia. We give the period, longitude, and latitude distributions corresponding to the first and second pole candidates (top and bottom rows, respectively).

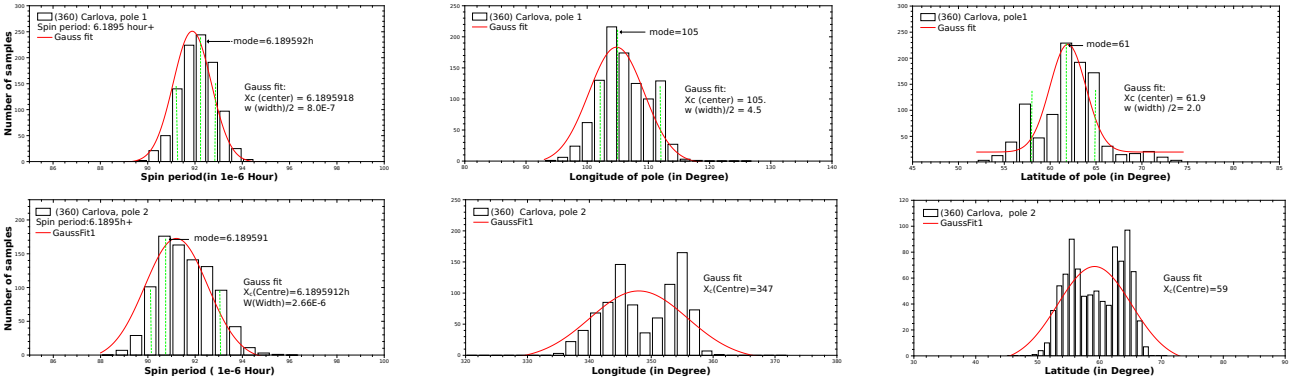

Fig. 8. The spin-parameter distributions for (360) Carlova. We give the period, longitude, and latitude distributions corresponding to the first and second pole candidates (top and bottom rows, respectively).

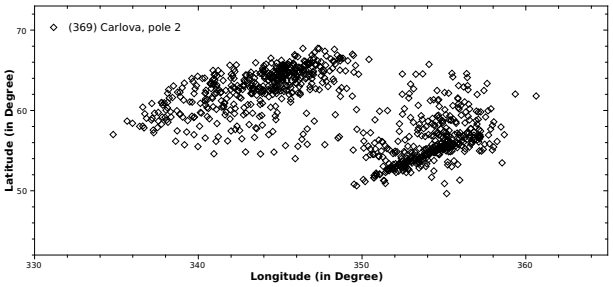

Fig. 10. The pole 2's distribution of (360) Carlova.

The convex shape of (360)Carlova is roughly close to a triaxial ellipsoid. Comparing to the axial ratios of Dotto et al.(1995), the new estimated axial ratio a/b is smaller and b/c is larger.

With the noval virtual-photometry Monte Carlo method, the uncertainties, as well as the most likely values of spin parameters can be investigated in the parameter space as long as enough samples can be computed for parameters. From the analysis results for two C-type asteroids, the pole uncertainties for the two asteroids are 5 degrees (full 1-σ width), and that of spin periods are less than 5×10^{-6} hours. The pole uncertainties of (360) Carlova are larger than those of (171) Ophelia, at least partly, because of the larger observational errors in parts of the photometric data for (360) Carlova.

Acknowledgements. This work was supported by National Natural Sciences Foundations of China (contracts No. 11073051 and No. 10933004). We'd like to thank the the project of exchange visit between Academy of Finland and Chinese Aademy of Sciences for providing the financial supports.

References

Bessell, M.S., Castelli, F., & Plez, B. 1998, A&A, 333, 231
Cellino, A., Zappalà, V., & Farinella, P. 1989, Icarus, 78, 298
Collier Cameron, A., and 24 colleagues 2006, MNRAS, 373,799
Di Martino, M., Zappalà, V., De Campos, J. A., Debehogne, H., & Lagerkvist, C.-I. 1987, A&A Suppl. Ser., 67, 95
Dotto, E., De Angelis, G., Di Martino, M., Barucci, M. A., Fulchignoni, M., De Sanctis, G., and Burchi, R. 1995, Icarus, 117, 313
Ďurech, J., Kaasalainen, M., Warner, B. D., Fauerbach, M., Marks, S. A., Fauvaud, S., Fauvaud, M., Vugnon, J.-M., Pilcher, F., Bernasconi, L., & Behrend, R. 2009, A&A, 493, 291
Ďurech, J., Sidorin, V., & Kaasalainen, M. 2010, A&A, 513, A46
Hanuš, J., Ďurech, J., Brož, M., Warner, B. D., Pilcher, F., Stephens, R., Oey, J., Bernasconi, L., Casulli, S., Behrend, R. and 5 coauthors 2011, A&A, 530, A134
Harris, A.W., & Young, J.W. 1983, Icarus, 54, 59
Karttunen, H. 1989, A&A, 208, 314
Karttunen, H., & Bowell, E. 1989, A&A, 208, 320
Kaasalainen, M., Lamberg, L., Lumme, K., Bowell, E. 1992, A&A 259, 318
Kaasalainen, M., Lamberg, L. & Lumme, K. 1992, A&A, 259, 333
Kaasalainen, M., & Torppa, J. 2001 Icarus, 153, 24
Kaasalainen, M., Torppa, J. & Muinonen K. 2001, Icarus, 153, 37
Kaasalainen, M., Torppa, J. & Piironen J. 2002, Icarus, 159, 369
Kaasalainen, M., Torppa, J. & Piironen, J. 2002, A&A, 383,L19
Kaasalainen, M., Pravec, P., Krugly, Y. N., Šarounová, L., Torppa, J., Virtanen, J., Kaasalainen, S., Erikson, A., Nathues, A., Ďurech, J., and 12 coauthors 2004, Icarus, 167 178
Michalowski, T., Pych, W., Berthier, J., A. Kryszczyńska, A., Kwiatkowski, T., Boussuge, J., Fauvaud, S., Denchev, P., & Baranowski, R. 2000, A&A Suppl. Ser., 146, 471
Muinonen, K. 1998, A&A, 332, 1087

Muinonen, K., &. Lagerros, J.S.V. 1998, A&A, 333, 753
Muinonen, K., Granvik, M., Oszkiewicz, D., Pieniluoma, T., & Pentikäinen, H. 2012, P&SS, 73, 15.
Russell, H. N. 1906, APJ, 24,1.
Tedesco, E. F. 1979, Science, 203, 905
Tamuz, O., Mazeh, T., & Zucher, S. 2005, MNRAS, 356,1466
Torppa, J., Kaasalainen, M., Michalowski, T., Kwiatkowski, T., Kryszczyńska, A., Denchev, P., & Kowalski, R. 2003, Icarus, 164, 346
Torppa, J., Hentunen, V.-P., Pääkkönen, P., Kehusmaa, P., Muinonen, K. 2008, Icarus, 198, 91
Wang, X.-b., & Zhang, X-l. 2006, CAA, 30, 410
Wang, X.-b., Gu, S.-h., & Li, X.-j. 2010, EM&P, 106, 97

Table 1. Description of observational data for (171) Ophelia and (360) Carlova. The following entries are included: the date in UTC (column 1); the geocentric and heliocentric distances of the asteroid (columns 2 and 3); the solar phase angle (column 4); the geocentric ecliptic coordinates of the asteroid (column 5); the filter (column 6); the observatory code assigned by the IAU Minor Planet Center (column 7); and a note marking the source of the data (column 8).

UTC date	Δ AU	r AU	Phase Deg.	Ecliptic coordinates in J2000.0	Filter	Observatory code	Note
(171) Ophelia							
1977 01 16.30	2.835	1.858	2.86	(121.717, 0.907)	V	049	published in Tedesco(1979)
2003 11 25.63	3.210	2.256	5.37	(50.693, -1.948)	R	286	observed by Xiaobin Wang
2003 11 30.67	3.204	2.277	7.09	(51.541, -1.923)	R	286	observed by Xiaobin Wang
2003 12 01.57	3.203	2.281	7.39	(51.693, -1.919)	R	286	observed by Xiaobin Wang
2003 12 02.63	3.202	2.286	7.74	(51.872, -1.914)	R	286	observed by Xiaobin Wang
2005 03 17.94	2.739	1.944	14.92	(147.223, 1.850)	Clear	938	observed by Rui Goncalves
2005 04 07.89	2.735	2.163	19.47	(152.064, 1.991)	Clear	938	observed by Rui Goncalves
2005 04 08.88	2.734	2.175	19.62	(152.294, 1.997)	Clear	938	observed by Rui Goncalves
2005 04 22.90	2.733	2.347	21.12	(155.540, 2.083)	Clear	938	observed by Rui Goncalves
2005 04 24.91	2.733	2.372	21.26	(156.007, 2.095)	Clear	938	observed by Rui Goncalves
2005 03 16.94	2.739	1.935	14.64	(146.992, 1.843)	R	132	observed by Pierre Antonini
2005 03 17.92	2.739	1.944	14.92	(147.219, 1.850)	R	132	observed by Pierre Antonini
2005 04 05.91	2.735	2.140	19.16	(151.606, 1.978)	R	132	observed by Pierre Antonini
2005 04 12.84	2.734	2.222	20.15	(153.210, 2.022)	R	132	observed by Pierre Antonini
2005 04 21.90	2.733	2.334	21.05	(155.309, 2.077)	R	132	observed by Pierre Antonini
2005 04 13.83	2.734	2.234	20.27	(153.439, 2.028)	R	A12	observed by Federico Manzini
2005 04 17.83	2.733	2.283	20.70	(154.366, 2.053)	R	A12	observed by Federico Manzini
2006 03 09.62	2.938	2.548	19.21	(226.425, 2.063)	R	E17	observed by Julian Oey
2006 03 12.65	2.942	2.511	18.97	(227.033, 2.047)	R	E17	observed by Julian Oey
2006 03 26.61	2.958	2.347	17.21	(229.811, 1.972)	R	E17	observed by Julian Oey
2006 03 27.57	2.959	2.336	17.05	(230.000, 1.966)	R	E17	observed by Julian Oey
2006 04 01.61	2.965	2.282	16.13	(230.994, 1.938)	R	E17	observed by Julian Oey
2006 04 05.58	2.970	2.243	15.29	(231.775, 1.915)	R	E17	observed by Julian Oey
2005 04 20.88	2.733	2.321	20.97	(155.073, 2.071)	R	511	observed by Yassine Damerdji
2005 04 21.89	2.733	2.334	21.05	(155.307, 2.077)	R	511	observed by Yassine Damerdji
2005 05 01.87	2.732	2.462	21.57	(157.621, 2.135)	R	809	observed by Alain Klotz& Raoul Behrend
2006 04 29.11	2.999	2.063	8.60	(236.348, 1.776)	V	586	observed by Arnand Leroy & Giller Ganand
2006 04 28.07	2.997	2.069	8.96	(236.146, 1.782)	Clear	938	observed by Rui Goncalves
2006 04 29.06	2.999	2.064	8.62	(236.338, 1.776)	Clear	938	observed by Rui Goncalves
2006 04 30.03	3.000	2.059	8.29	(236.525, 1.770)	Clear	938	observed by Rui Goncalves
2006 05 01.07	3.001	2.054	7.93	(236.723, 1.763)	Clear	938	observed by Rui Goncalves
2006 05 25.00	3.031	2.020	1.41	(241.277, 1.612)	R	938	observed by Rui Goncalves
2006 07 19.89	3.102	2.496	16.86	(251.560, 1.235)	R	938	observed by Rui Goncalves
2011 04 09.98	2.778	1.794	4.88	(191.236, 2.546)	V	J23	observed by Jacques Montier
2011 04 22.94	2.787	1.860	9.79	(194.134, 2.541)	V	J23	observed by Jacques Montier
2011 04 20.91	2.786	1.847	9.06	(193.680, 2.543)	B	B91	Observed by Charistophe Demeautis
2011 04 21.94	2.786	1.853	9.43	(193.911, 2.542)	B	B91	Observed by Charistophe Demeautis
2011 04 22.92	2.787	1.860	9.78	(194.129, 2.541)	B	B91	Observed by Charistophe Demeautis
2011 04 25.95	2.789	1.881	10.84	(194.804, 2.539)	V	B91	Observed by Charistophe Demeautis
2011 04 26.84	2.790	1.888	11.14	(195.001, 2.539)	V	B91	Observed by Charistophe Demeautis
(360) Carlova							
1979 10 25.24	2.613	1.735	12.61	(11.352, -9.9537)	V	645	published in Harris(1983)
1979 10 26.13	2.612	1.740	12.91	(11.573, -9.9773)	V	645	published in Harris(1983)
1979 10 27.24	2.610	1.747	13.25	(11.849, -10.0063)	V	645	published in Harris(1983)
1979 10 28.27	2.609	1.754	13.58	(12.107, -10.0333)	V	645	published in Harris(1983)
1984 09 21.18	2.797	1.846	8.13	(344.861, -6.2672)	V	809	published in Di Martino(1987)
1984 09 22.21	2.795	1.850	8.50	(345.079, -6.3050)	V	809	published in Di Martino(1987)
1986 01 09.95	2.588	1.611	3.15	(108.151, -4.9495)	V	022	published in Dotto(1995)
1996 01 19.91	2.463	1.951	22.10	(71.781, -10.2650)	R	586	published in Michalowski(2000)
1997 03 03.01	3.038	2.058	3.50	(165.885, 6.4625)	V	071	published in Michalowski(2000)
1997 03 04.01	3.040	2.059	3.35	(166.067, 6.4935)	V	071	published in Michalowski(2000)
1997 03 10.99	3.052	2.071	3.55	(167.320, 6.7060)	Clear	187	published in Michalowski(2000)
1998 04 27.98	3.527	2.583	6.69	(230.594, 11.5971)	Clear	187	published in Michalowski(2000)
1998 04 30.98	3.528	2.572	6.05	(231.007, 11.5855)	Clear	187	published in Michalowski(2000)
1998 05 02.96	3.528	2.565	5.67	(231.280, 11.5776)	Clear	187	published in Michalowski(2000)
2000 11 15.63	2.496	1.629	13.54	(33.903, -11.5703)	R	286	published in Wang(2004)
2011 11 02.82	2.522	2.091	22.45	(93.097, -7.5004)	Clear	286	observed by Wang Xiaobin
2011 11 26.81	2.547	1.840	18.30	(99.334, -6.4764)	Clear	286	observed by Wang Xiaobin
2011 11 27.85	2.548	1.830	18.04	(99.601, -6.4306)	Clear	286	observed by Wang Xiaobin
2011 12 17.73	2.572	1.683	11.62	(104.646, -5.5403)	Clear	286	observed by Wang Xiaobin
2011 12 18.77	2.573	1.677	11.22	(104.906, -5.4931)	Clear	286	observed by Wang Xiaobin
2012 01 23.78	2.622	1.662	5.90	(113.745, -3.8243)	Clear	286	observed by Wang Xiaobin
2012 03 11.59	2.696	2.135	19.68	(124.902, -1.5846)	R	286	observed by Wang Xiaobin
2012 03 12.55	2.698	2.148	19.81	(125.118, -1.5403)	R	286	observed by Wang Xiaobin
2012 03 17.58	2.706	2.218	20.39	(126.2514, -1.307)	R	286	observed by Wang Xiaobin